

# Critical behaviour of the $O(3)$ nonlinear sigma model with topological term at $\theta = \pi$ from numerical simulations

Vicente Azcoiti<sup>a\*</sup>, Giuseppe Di Carlo<sup>b†</sup>, Eduardo Follana<sup>a‡</sup>,  
and Matteo Giordano<sup>a§</sup>

<sup>a</sup> Departamento de Física Teórica, Universidad de Zaragoza,  
Calle Pedro Cerbuna 12, E-50009 Zaragoza, Spain

<sup>b</sup> INFN, Laboratori Nazionali del Gran Sasso,  
I-67010 Assergi (L'Aquila), Italy

## Abstract

We investigate the critical behaviour at  $\theta = \pi$  of the two-dimensional  $O(3)$  nonlinear sigma model with topological term on the lattice. Our method is based on numerical simulations at imaginary values of  $\theta$ , and on scaling transformations that allow a controlled analytic continuation to real values of  $\theta$ . Our results are compatible with a second order phase transition, with the critical exponent of the  $SU(2)_1$  Wess-Zumino-Novikov-Witten model, for sufficiently small values of the coupling.

---

\*E-mail: azcoiti@azcoiti.unizar.es

†E-mail: giuseppe.dicarlo@lngs.infn.it

‡E-mail: efollana@unizar.es

§E-mail: giordano@unizar.es

# 1 Introduction

Quantum field theories with a topological term (“ $\theta$ -term”) in the action have proved to be particularly challenging to investigate. Such theories are related to a few important open problems in theoretical physics, including the so-called “strong  $CP$  problem” in strong interactions, and to interesting phenomena in condensed matter physics, such as the quantum Hall effect (for a recent review on theories with  $\theta$ -term, see Ref. [1]).

On the one hand, topological properties are intrinsically nonperturbative, thus requiring a nonperturbative approach to the study of these systems. On the other hand, the most effective of these approaches, namely the numerical study by means of simulations in lattice field theory, cannot be directly applied to these systems, due to the presence of a so-called *sign problem*. Infact, the complex nature of their Euclidean action prevents the computation of the relevant functional integrals by means of the usual importance-sampling techniques. Numerical investigations have then required the use of techniques which allow to avoid the sign problem, usually based on analytic continuation or on the resummation of the contributions of the various topological sectors to the partition function [2, 3, 4, 5, 6, 7, 8]. The basic idea of these techniques is to modify or split the functional integral, in such a way that the resulting expression(s) have a positive-definite integration measure, and therefore can be treated with the usual numerical techniques. The difficulty of dealing with an oscillatory integrand is however not completely overcome, but simply shifted to the problem of reconstructing the original functional integral, which is usually a very delicate issue from the numerical point of view. It is worth noting that, beside having their own theoretical interest, theories with a  $\theta$ -term share the sign problem with finite-density QCD, and so the development of techniques and algorithms to solve or by-pass the sign problem can have positive consequences on the study of the QCD phase diagram by means of numerical simulations.

Among the various existing models, the two-dimensional  $O(3)$  nonlinear sigma model with  $\theta$ -term ( $O(3)_\theta\text{NL}\sigma\text{M}$ ) deserves particular interest. It has been shown long ago by Haldane [9, 10] that chains of quantum spins with antiferromagnetic interactions, in the semiclassical limit of large but finite spin  $S$ , are related to this model at coupling  $g^2 = 4/[S(S+1)]$ , and at  $\theta = 0$  or  $\pi$  if the spin is respectively integer or half-integer. Haldane conjectured that quantum spin chains for half-integer spins show a gapless spectrum, and correspondingly that a second-order phase transition takes place in the  $O(3)_\theta\text{NL}\sigma\text{M}$  at  $\theta = \pi$ , with vanishing of the mass gap and recovery of parity. Arguments supporting this conjecture have been provided in Ref. [11]. Moreover, in Ref. [12] it has been argued that the critical theory for generic half-integer spin antiferromagnets is the  $SU(2)$  Wess-Zumino-Novikov-Witten (WZNW) model [13, 14, 15] at topological coupling  $k = 1$ , which in turn should determine the behaviour of the mass gap near  $\theta = \pi$ .

Numerical investigations of Haldane’s conjecture have been performed, following basically three different strategies. A first strategy [2, 16] is based on the determina-

tion of the probability distribution of the topological charge by means of simulations at  $\theta = 0$ , which allows in principle to reconstruct the expectation values of the various observables at  $\theta \neq 0$ . In order to achieve the very high accuracy required by this approach, the authors of Refs. [2, 16] have employed a constrained (“topological” [17]) action on a triangular lattice, which allows simulations by means of an efficient Wolff cluster algorithm [18]. The parameters of the action were chosen in order to be in the weak-coupling regime. Using finite size scaling theory, the authors of Ref. [2, 16] found a second order phase transition at  $\theta = \pi$ , in agreement with Haldane’s conjecture, and a finite size scaling in good agreement with the assumption of a WZNW-type of critical behaviour.

A second strategy [19] is based on the determination of the mass gap at imaginary values of  $\theta$ , that can be obtained directly by means of numerical simulations, and the subsequent analytic continuation to real values of  $\theta$ , in order to check if the mass gap vanishes at some point. The authors of Ref. [19] found indeed that the mass gap vanishes at  $\theta = \theta_c$  for some real  $\theta_c$ , and moreover that  $\theta_c = \pi$  within the errors, again in agreement with Haldane’s conjecture.

Finally, the third strategy [20, 21, 22, 23] makes use again of numerical simulations at imaginary values of  $\theta$ , in order to determine the topological charge density, and of a controlled way of performing the analytic continuation to real  $\theta$  that greatly reduces the uncertainties connected to this process. Applying this strategy to the  $CP^1$  model, that is expected to be equivalent to the  $O(3)$  model, the authors of Ref. [22] found a richer phase structure, with a first-order phase transition at  $\theta = \pi$  for  $\beta \lesssim 0.5$ , and a line of second-order phase transitions with recovery of parity for  $0.5 \lesssim \beta \lesssim 1.5$ , with continuously varying critical exponent. At  $\beta \simeq 1.5$  the critical exponent becomes 2, and parity is recovered analytically.

In this paper we want to investigate further on this issue, by applying the strategy of Refs. [20, 21, 22, 23] directly to the  $O(3)_\theta \text{NL}\sigma\text{M}$ . Our aim is to understand the origin of the discrepancy between the results of Refs. [2, 16] and those of Ref. [22]. Such a discrepancy could be of physical origin, due to the actual inequivalence of the  $O(3)$  and  $CP^1$  models, contrary to the standard wisdom; or it could be of technical origin, due to shortcomings of the employed strategy in dealing with these models. The plan of the paper is the following. In Section 2 we briefly review the method of Refs. [20, 21, 22, 23]. In Section 3 we describe the model of interest, discussing in particular the theoretical prediction for the critical behaviour of the model at  $\theta = \pi$  in the continuum, and working out the consequences for the observables relevant to our method. In Section 4 we describe the  $O(3)_\theta \text{NL}\sigma\text{M}$  on the lattice, and we discuss the results of our numerical simulations. Finally, Section 5 is devoted to our conclusions and to an outlook on open problems. Details of the numerical analysis are reported in the Appendix.

## 2 Theories with topological term in the action and the method of scaling transformations

In this Section we briefly describe the relevant formalism and notation that will be used in the rest of the paper. The partition function of a theory with a topological term in the action is of the general form

$$Z(\theta) = \int \mathcal{D}\phi e^{-S[\phi] + i\theta Q[\phi]} = e^{-VF(\theta)}, \quad (1)$$

where  $\phi$  denotes the degrees of freedom of the model,  $\mathcal{D}\phi$  is the appropriate functional measure,  $S$  is the non-topological part of the action, and  $Q$  is the quantised topological charge, taking only integer values; moreover,  $F(\theta)$  is the free energy density and  $V$  the volume of the system. Clearly,  $Z(\theta)$  is a periodic function of  $\theta$ ,  $Z(\theta + 2\pi) = Z(\theta)$ . In the interesting cases, the integration measure is invariant under parity ( $\mathcal{P}$ ), and  $S$  is  $\mathcal{P}$ -even, while  $Q$  is  $\mathcal{P}$ -odd. As a consequence,  $Z(-\theta) = Z(\theta)$ ; combining this with periodicity, we have that  $Z(\pi + \theta) = Z(\pi - \theta)$ .

While at  $\theta \neq 0, \pi$  parity is explicitly broken, at  $\theta = \pi$  any  $\mathcal{P}$ -odd observable has vanishing expectation value in a finite volume; nevertheless, a phase transition may take place at this point. A convenient order parameter is given by the topological charge density,

$$\mathbf{O}(\theta) \equiv -i \frac{\langle Q \rangle_{i\theta}}{V} = -\frac{1}{V} \frac{\partial \log Z(\theta)}{\partial \theta} = \frac{\partial F(\theta)}{\partial \theta}, \quad (2)$$

where we have introduced the notation

$$\langle \mathcal{O}[\phi] \rangle_{i\theta} = Z(\theta)^{-1} \int \mathcal{D}\phi e^{-S[\phi] + i\theta Q[\phi]} \mathcal{O}[\phi], \quad (3)$$

for the expectation value of the observable  $\mathcal{O}[\phi]$ . In the limit of infinite volume, a nonzero value of  $\mathbf{O}(\theta = \pi)$  indicates a first-order phase transition, while a divergent susceptibility  $\mathbf{O}'(\theta = \pi)$  indicates a second-order phase transition, and so on.

In order to reconstruct the behaviour of the order parameter near  $\theta = \pi$  using numerical simulations, one has to start from imaginary values of the vacuum angle  $\theta = -ih$ , with  $h \in \mathbb{R}$ . It has been suggested in Ref. [20] that a convenient observable is the quantity

$$y(z) = \frac{\langle Q \rangle_h}{V \tanh \frac{h}{2}}, \quad z = \cosh \frac{h}{2}, \quad z \geq 1. \quad (4)$$

It is immediate to see that under analytic continuation  $h \rightarrow i\theta$  one has

$$y(z) = -i \frac{\langle Q \rangle_{i\theta}}{V \tan \frac{\theta}{2}} = \frac{\mathbf{O}(\theta)}{\tan \frac{\theta}{2}}, \quad z = \cos \frac{\theta}{2}, \quad z \leq 1. \quad (5)$$

i.e., in terms of  $z$  the analytic continuation is simply an extrapolation from  $z \geq 1$  to  $z \leq 1$ . Notice that  $y(1) = \frac{2\langle Q^2 \rangle_h}{V}$ , and  $y(0) = 0$ , with  $z = 0$  corresponding to  $\theta = \pi$ .<sup>1</sup>

---

<sup>1</sup>One can have  $y(0) \neq 0$  only if the topological charge density diverges at  $\theta = \pi$ , which seems unlikely.

The use of this observable is suggested by the antiferromagnetic one-dimensional Ising model, where the role of the  $\theta$ -term is played by the coupling with an external imaginary magnetic field (for an even number of sites). This model is exactly solvable, and one finds that  $y$  actually depends only on a specific combination of  $z$  and of the antiferromagnetic coupling  $F$ , namely  $y(z, F) = Y((e^{-4F} - 1)^{-\frac{1}{2}} z)$ . Although this property is exclusive of the one-dimensional Ising model, nevertheless one can expect that a similar smooth relation exists between  $y(z)$  and  $y_\lambda(z) \equiv y(e^{\frac{\lambda}{2}} z)$  also in other models with  $\theta$ -term. The assumption usually made is that  $y(z)$  is a monotonically increasing function of  $z$ , vanishing only for  $z = 0$  (i.e., the order parameter does not vanish for  $\theta \in (0, \pi)$ ); this is indeed the case for the models where the exact solution is known. The quantity  $y_\lambda$  is then a monotonic function  $y_\lambda(y)$  of  $y$ , with the property that  $y_\lambda = 0$  at  $y = 0$ , so that starting from the smallest values of  $y$  that can be obtained by numerical simulations at real  $h$ , one can therefore reliably extrapolate towards  $y = y_\lambda = 0$ , i.e., in the region corresponding to real  $\theta = -ih$ . This is the advantage of this method, based on scaling transformation, over other approaches that involve an uncontrolled analytic continuation from imaginary values of  $\theta$ . Having reconstructed  $y_\lambda(y)$  in this region, one can then easily reconstruct the order parameter at real  $\theta$ . Clearly, the closer one gets to  $y = 0$ , the better the extrapolation is expected to be: this method is then expected to work well in situations where the density of topological objects is small, such as asymptotically free models at weak coupling.

If one is interested only in the critical behaviour at  $\theta = \pi$ , it is possible to determine the critical exponent without explicitly reconstructing the order parameter. Consider the effective exponent  $\gamma_\lambda(y)$ ,

$$\gamma_\lambda(y) \equiv \frac{2}{\lambda} \log \frac{y_\lambda(y)}{y}. \quad (6)$$

Assuming a critical behaviour  $\mathbf{O} \propto z^\epsilon$  near  $z = 0$ , i.e.,  $\mathbf{O} \propto (\pi - \theta)^\epsilon$  near  $\theta = \pi$ , one immediately sees that  $y \propto z^{\epsilon+1}$  near  $z = 0$ , and so

$$\gamma \equiv \lim_{y \rightarrow 0} \gamma_\lambda(y) = \frac{2}{\lambda} \lim_{z \rightarrow 0} \log \frac{e^{(1+\epsilon)\frac{\lambda}{2}} z^{1+\epsilon}}{z^{1+\epsilon}} = 1 + \epsilon. \quad (7)$$

Analogously, assuming that  $y_\lambda(y)$  is analytic at  $y = 0$ , one can obtain  $\gamma$  from the relation  $\gamma = \frac{2}{\lambda} \log \left( \frac{dy_\lambda}{dy} \Big|_{y=0} \right)$ .

The method outlined above has been checked against explicitly solvable models, and successfully applied to models where the exact solution is not known (see Refs. [20, 21, 22, 23]). One implicit assumption of this method is that the function  $y_\lambda(y)$  has a “reasonable” behaviour near  $y = 0$ , i.e., it can be well approximated by polynomials, or ratios of polynomials, or other “simple” functions. If this is the case, the critical exponent can then be obtained with fair accuracy. What has not been done yet is the evaluation of the impact of logarithmic corrections on the reliability of the extrapolation. The result Eq. (7) holds independently of logarithmic corrections to the critical behaviour, i.e., it holds even if  $\mathbf{O} \propto z^\epsilon \log(1/z)^{-\beta}$ ; nevertheless,

the way in which the limit is approached in this case can make the extrapolation more difficult. This issue will be discussed further on in the next Section.

### 3 The $O(3)$ nonlinear sigma model with a topological term

In this Section we briefly recall the main properties of the  $O(3)$  nonlinear sigma model with a topological term ( $O(3)_\theta \text{NL}\sigma\text{M}$ ) in two dimensions, and we work out the consequences of the expected critical behaviour at  $\theta = \pi$  for the method of scaling transformations described in the previous Section.

#### 3.1 Critical behaviour at $\theta = \pi$

The degrees of freedom of the  $O(3)_\theta \text{NL}\sigma\text{M}$  in two dimensions are real three-component spin variables  $\vec{s}(x)$  of modulus one,  $\vec{s}(x)^2 = 1$ , “living” at the point  $x \in \mathbb{R}^2$ . Expectation values are defined in terms of functional integrals as follows,

$$\langle \mathcal{O}[\vec{s}] \rangle_{i\theta} \equiv Z(\theta)^{-1} \int \mathcal{D}\vec{s} e^{-S[\vec{s}] + i\theta Q[\vec{s}]} \mathcal{O}[\vec{s}], \quad Z(\theta) = \int \mathcal{D}\vec{s} e^{-S[\vec{s}] + i\theta Q[\vec{s}]}, \quad (8)$$

where the measure is given by  $\mathcal{D}\vec{s} = \prod_x d^3\vec{s}(x) \delta(1 - \vec{s}(x)^2)$ . In the continuum,

$$S[\vec{s}] = \frac{1}{2g^2} \int d^2x \partial_\mu \vec{s}(x) \cdot \partial_\mu \vec{s}(x), \quad (9)$$

and the topological charge  $Q[\vec{s}]$  is given by

$$Q[\vec{s}] = \frac{1}{8\pi} \int d^2x \vec{s}(x) \cdot \epsilon^{\mu\nu} \partial_\mu \vec{s}(x) \wedge \partial_\nu \vec{s}(x). \quad (10)$$

Here  $\mu, \nu = 1, 2$ , and sum over repeated indices is understood; the antisymmetric symbol  $\epsilon^{\mu\nu}$  is defined as  $\epsilon^{12} = -\epsilon^{21} = 1$ ,  $\epsilon^{11} = \epsilon^{22} = 0$ .

While at  $\theta = 0$  the theory possesses a mass gap, it has been argued that as  $\theta \rightarrow \pi$  the mass gap  $m(\theta)$  vanishes with the following behaviour [24]:

$$m(\theta) \propto |\pi - \theta|^{\frac{2}{3}} \left| \log \frac{1}{|\pi - \theta|} \right|^{-\frac{1}{2}} \underset{\theta < \pi, \theta \simeq \pi}{=} (\pi - \theta)^{\frac{2}{3}} \left( \log \frac{1}{\pi - \theta} \right)^{-\frac{1}{2}}, \quad (11)$$

where we have neglected subleading terms.<sup>2</sup> This prediction follows from the following considerations for the continuum theory (see Refs. [12, 24, 25]). Near  $\theta = \pi$ , the effective action for the  $O(3)$  sigma model is given by the  $SU(2)_1$  Wess-Zumino-Novikov-Witten (WZNW) model [13, 14, 15], with a marginally irrelevant, parity-preserving perturbation, and a relevant, parity-breaking perturbation, whose coupling  $\tilde{g}$  is a function of  $(\pi - \theta)$  that vanishes at  $\theta = \pi$ . Renormalisation-group

---

<sup>2</sup>From now on we will work in the interval  $\theta \in [0, \pi]$ , so that we can discard the absolute values.

arguments relate as follows the coupling and the correlation length  $\xi$  of the system [24],

$$\frac{1}{\tilde{g}} \propto \xi^{\frac{3}{2}} (\log \xi)^{-\frac{3}{4}} \times [1 + \mathcal{O}((\log \xi)^{-1})] ; \quad (12)$$

neglecting subleading terms, as  $m \propto \xi^{-1}$ , one finds

$$m \propto \tilde{g}^{\frac{2}{3}} \left( \log \frac{1}{\tilde{g}} \right)^{-\frac{1}{2}} . \quad (13)$$

It is usually assumed that  $\tilde{g} \propto (\pi - \theta) + \dots$ , so that Eq. (11) immediately follows.

Following Kadanoff, one expects that near the critical point  $\theta = \pi$  the free energy density  $F(\theta)$  is proportional to the square of the inverse of the correlation length, that in turn is proportional to the inverse mass gap, so that

$$F(\theta) \propto \frac{1}{\xi(\theta)^2} \propto m(\theta)^2 . \quad (14)$$

The order parameter for parity breaking  $\mathbf{O}(\theta)$ , defined in Eq. (2), is therefore expected to show the following behaviour near  $\theta = \pi$ ,

$$\mathbf{O}(\theta) \propto \frac{\partial m(\theta)^2}{\partial \theta} \propto (\pi - \theta)^{\frac{1}{3}} \left( \log \frac{1}{\pi - \theta} \right)^{-1} , \quad (15)$$

where we have neglected subleading terms. This behaviour is conveniently rewritten as follows in terms of the variable  $z = \cos \frac{\theta}{2}$  ( $z \leq 1$ ),

$$\mathbf{O}(\theta) \propto z^{\frac{1}{3}} \left( \log \frac{1}{z} \right)^{-1} , \quad z \ll 1 . \quad (16)$$

The critical behaviour is therefore a second-order phase transition, with recovery of parity, with a critical exponent  $\epsilon = \frac{1}{3}$ .

For future utility, it is useful to work out the first correction to the leading behaviour Eq. (13). This does not require the knowledge of the  $\mathcal{O}((\log \xi)^{-1})$  terms in Eq. (12); we have

$$m \propto \tilde{g}^{\frac{2}{3}} \left( \log \frac{1}{\tilde{g}} \right)^{-\frac{1}{2}} \left[ 1 - \frac{3}{8} \frac{\log \log \frac{1}{\tilde{g}}}{\log \frac{1}{\tilde{g}}} + \frac{1}{\log \frac{1}{\tilde{g}}} r \left( \log \frac{1}{\tilde{g}} \right) \right] , \quad (17)$$

where the function  $r(x)$  is of the form  $r(x) = r_0 + (r_1 \log(x) + r_2)/x + \dots$ , and we have omitted subleading terms at large  $x$ . We will assume that subleading terms in the relation  $\tilde{g} \propto (\pi - \theta) + \dots$  are suppressed as powers of  $\pi - \theta$ , so that they can be safely ignored in the analysis of the following subsections. Using Eq. (17), we find for the order parameter

$$\mathbf{O} \propto z^{\frac{1}{3}} \left( \log \frac{1}{z} \right)^{-1} \left[ 1 - \frac{3}{4} \frac{\log \log \frac{1}{z}}{\log \frac{1}{z}} + \frac{1}{\log \frac{1}{z}} \tilde{r} \left( \log \frac{1}{z} \right) \right] , \quad (18)$$

where again  $\tilde{r}(x)$  is of the form  $\tilde{r}(x) = \tilde{r}_0 + (\tilde{r}_1 \log(x) + \tilde{r}_2)/x + \dots$

### 3.2 Effect of logarithmic corrections on the effective exponent. Extension of the method

We can now work out how the predicted behaviour of the order parameter near the critical point reflects on the effective exponent  $\gamma_\lambda$  defined in Eq. (6). Using Eq. (18), one finds that near  $z = 0$  the quantity  $y(z)$  has the following behaviour:

$$y(z) = y_0 z^{\frac{4}{3}} \left( \log \frac{1}{z} \right)^{-1} c(z), \quad (19)$$

where  $y_0$  is some constant and  $c(z) = 1 - \frac{3}{4} \frac{\log \log \frac{1}{z}}{\log \frac{1}{z}} + \dots$  (see Eq. (18)), where the dots stand for subleading terms. We have therefore for  $y_\lambda(z)$

$$\begin{aligned} y_\lambda(z) &= e^{\frac{\lambda}{2} \frac{4}{3}} y_0 z^{\frac{4}{3}} \left( \log \frac{1}{z} - \frac{\lambda}{2} \right)^{-1} c(e^{\frac{\lambda}{2}} z) \\ &= e^{\frac{\lambda}{2} \frac{4}{3}} y_0 z^{\frac{4}{3}} \left( \log \frac{1}{z} \right)^{-1} \left( 1 + \frac{\lambda}{2} \frac{1}{\log \frac{1}{z}} + \dots \right) c(e^{\frac{\lambda}{2}} z) \\ &= e^{\frac{\lambda}{2} \frac{4}{3}} \left( 1 + \frac{\lambda}{2} \frac{1}{\log \frac{1}{z}} + \dots \right) y(z), \end{aligned} \quad (20)$$

and so

$$\gamma_\lambda(y) = \frac{4}{3} + \frac{2}{\lambda} \log \left( 1 + \frac{\lambda}{2} \frac{1}{\log \frac{1}{z}} \right) + \dots = \frac{4}{3} + \frac{1}{\log \frac{1}{z}} + \dots \quad (21)$$

Taking the logarithm on both sides of Eq. (19), we find to leading order  $\log \frac{1}{z} = \frac{3}{4} \log \frac{1}{y(z)} + \dots$ , and plugging this into Eq. (21) we finally obtain

$$\gamma_\lambda(y) = \frac{4}{3} \left( 1 + \frac{1}{\log \frac{1}{y}} \right) + o \left( \frac{1}{\log \frac{1}{y}} \right). \quad (22)$$

The derivative of this function is infinite at the origin: as a consequence, the effective exponent changes abruptly at very small  $y$ , going from  $\gamma_\lambda \simeq \frac{4}{3} \simeq 1.33$  at  $y = 0$  to  $\gamma_\lambda \simeq 1.43$  at  $y = 10^{-6}$  (see Fig. 1). From a practical point of view, this behaviour makes it very hard to obtain the correct extrapolation from numerical data: one would need high precision data at very small values of  $y$  in order to figure out the logarithmic behaviour.

It is possible to modify the method of scaling transformations discussed above, in order to reduce the effect of the logarithmic corrections. Indeed, it suffices to consider a new function  $\bar{y}(z)$ , obtained by multiplying  $y$  by an appropriate factor, designed to cancel the logarithmic corrections at  $\theta = \pi$ . A convenient choice is

$$\bar{y}(z) \equiv y(z) \cosh \frac{h}{2} \log \left( 1 + \frac{1}{\cosh \frac{h}{2}} \right) = \frac{\langle Q \rangle_h}{V \tanh \frac{h}{2}} \cosh \frac{h}{2} \log \left( 1 + \frac{1}{\cosh \frac{h}{2}} \right). \quad (23)$$



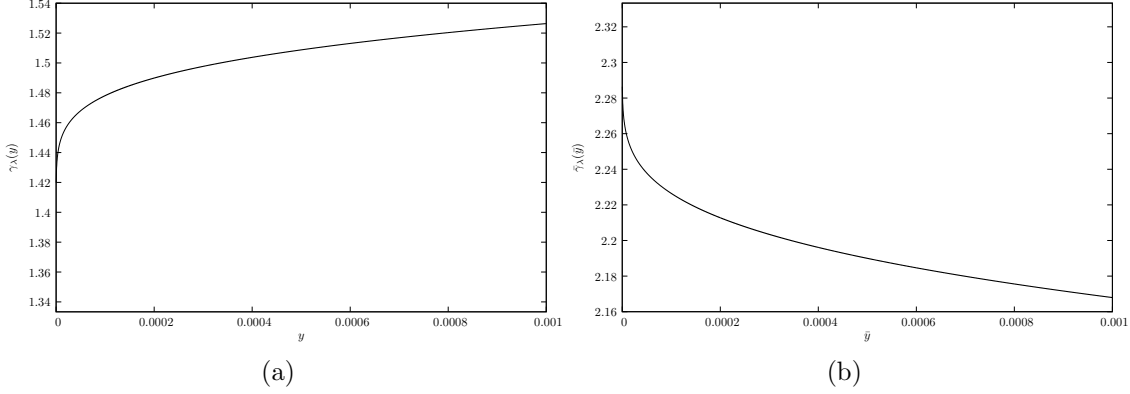


Figure 1: (a) Theoretical prediction for  $\gamma_\lambda(y)$  up to order  $\mathcal{O}\left(\log \frac{1}{y(z)}\right)$ .  
(b) Theoretical prediction for  $\bar{\gamma}_\lambda(\bar{y})$  up to order  $\mathcal{O}\left(\frac{\log \log \frac{1}{\bar{y}(z)}}{(\log \frac{1}{\bar{y}(z)})^2}\right)$ .

It is immediate to show that the extra term behaves as

$$\cosh \frac{h}{2} \log \left(1 + \frac{1}{\cosh \frac{h}{2}}\right) \xrightarrow{h \rightarrow i\theta} \cos \frac{\theta}{2} \log \left(1 + \frac{1}{\cos \frac{\theta}{2}}\right) \xrightarrow{\theta \rightarrow \pi} z \log \frac{1}{z}; \quad (24)$$

therefore, near  $z = 0$  we have that  $\bar{y}(z) \propto z^{\frac{7}{3}}$ , without logarithmic corrections.<sup>3</sup> Compared to similar functions yielding the desired logarithmic term, this choice has the advantage that the behaviour Eq. (24) of the extra factor has only corrections of order  $\mathcal{O}(z^2)$  near  $z = 0$ , and that the large- $h$  behaviour of  $\bar{y}$  is the same as that of the topological charge density, so avoiding possible distortions in the numerical analysis. Moreover, the extra factor is a monotonically increasing function of  $z$ , so that it cannot modify the monotonicity properties of  $y(z)$  (which is assumed to be a monotonically increasing function for the whole method to work).

It is straightforward now to work out the theoretical prediction for the behaviour of the new effective exponent

$$\bar{\gamma}_\lambda(\bar{y}) \equiv \frac{2}{\lambda} \log \frac{\bar{y}_\lambda}{\bar{y}}. \quad (25)$$

Clearly,

$$\bar{\gamma} \equiv \lim_{\bar{y} \rightarrow 0} \bar{\gamma}_\lambda(\bar{y}) = \gamma + 1 = \epsilon + 2 = \frac{7}{3}. \quad (26)$$

---

<sup>3</sup> More generally, if the order parameter behaves as  $\mathbf{O} \propto z^\epsilon (\log \frac{1}{z})^{-\rho}$ , one can define

$$\bar{y}(z, \rho) = \frac{\langle Q \rangle_h}{V \tanh \frac{h}{2}} \left[ \cosh \frac{h}{2} \log \left(1 + \frac{1}{\cosh \frac{h}{2}}\right) \right]^\rho.$$

in order to take care of logarithmic factors. One has that  $\bar{y}(z, \rho) \propto z^{\epsilon+1+\rho}$  near  $z = 0$ , without logarithmic corrections.

Near  $z = 0$ , we have that (see Eq. (18))

$$\bar{y}(z) = \bar{y}_0 z^{\frac{7}{3}} \left[ 1 - \frac{3}{4} \frac{\log \log \frac{1}{z}}{\log \frac{1}{z}} + \dots \right], \quad (27)$$

where  $\bar{y}_0$  is some constant, and also

$$\begin{aligned} \bar{\gamma}_\lambda(z) &= e^{\frac{\lambda}{2} \frac{7}{3}} \bar{y}_0 z^{\frac{7}{3}} \left[ 1 - \frac{3}{4} \frac{\log(\log \frac{1}{z} - \frac{\lambda}{2})}{\log \frac{1}{z} - \frac{\lambda}{2}} + \dots \right] \\ &= e^{\frac{\lambda}{2} \frac{7}{3}} \bar{y}_0 z^{\frac{7}{3}} \left[ 1 - \frac{3}{4} \left( \frac{\log \log \frac{1}{z}}{\log \frac{1}{z}} + \frac{\lambda}{2} \frac{\log \log \frac{1}{z}}{\log \frac{1}{z}} + \dots \right) + \dots \right] \\ &= e^{\frac{\lambda}{2} \frac{7}{3}} \left[ 1 - \frac{3}{4} \frac{\lambda \log \log \frac{1}{z}}{2 (\log \frac{1}{z})^2} + \dots \right] \bar{y}(z), \end{aligned} \quad (28)$$

where the neglected terms in the last passage are of order  $\mathcal{O}([\log(1/z)]^{-2})$ . Taking logarithms on both sides of Eq. (27) one immediately sees that to leading order  $\log \frac{1}{z} = \frac{3}{7} \log \frac{1}{\bar{y}} + \dots$ , and so one finds that<sup>4</sup>

$$\bar{\gamma}_\lambda(\bar{y}) = \frac{7}{3} - \frac{49}{12} \frac{\log \log \frac{1}{\bar{y}}}{(\log \frac{1}{\bar{y}})^2} + \dots \quad (29)$$

Although there still are logarithmic effects in the approach to the limit value, the “jump” of the function between  $\bar{y} = 0$  and  $\bar{y} = 10^{-6}$  is half as much as that of  $\gamma_\lambda$  predicted above (see Fig. 1). Moreover, it is easy to see that corrections to the leading-order relation between  $\log \frac{1}{z}$  and  $\log \frac{1}{\bar{y}}$  are vanishing as  $\bar{y} \rightarrow 0$ , i.e.,  $\log \frac{1}{z} = \frac{3}{7} \log \frac{1}{\bar{y}} + o(1)$ , while in the relation between  $\log \frac{1}{z}$  and  $\log \frac{1}{y}$  there are also subleading but divergent terms as  $y \rightarrow 0$ . The bottom line is that the use of  $\bar{\gamma}_\lambda$  and  $\bar{y}$  instead of  $\gamma_\lambda$  and  $y$  is expected to improve the numerical analysis.

In concluding this Section, we want to add a few remarks. First of all, we want to stress that the results of this Section are expected to hold in the continuum limit, and they are based on the fundamental assumption that the critical theory at  $\theta = \pi$  is the  $SU(2)$  WZNW model at topological coupling  $k = 1$ . We notice also that the prediction for the quantity  $\bar{y}(z)$  has been derived using the behaviour of the mass gap near the critical point  $\theta = \pi$ , i.e., near  $z = 0$ , so that it is not expected to hold for  $z \geq 1$ , where numerical simulations are feasible. On the other hand, due to its expected smoothness, the prediction for  $\bar{\gamma}_\lambda(\bar{y})$  should hold more generally in the region of small  $\bar{y}$ , that is accessible to numerical simulations at sufficiently small values of the coupling.

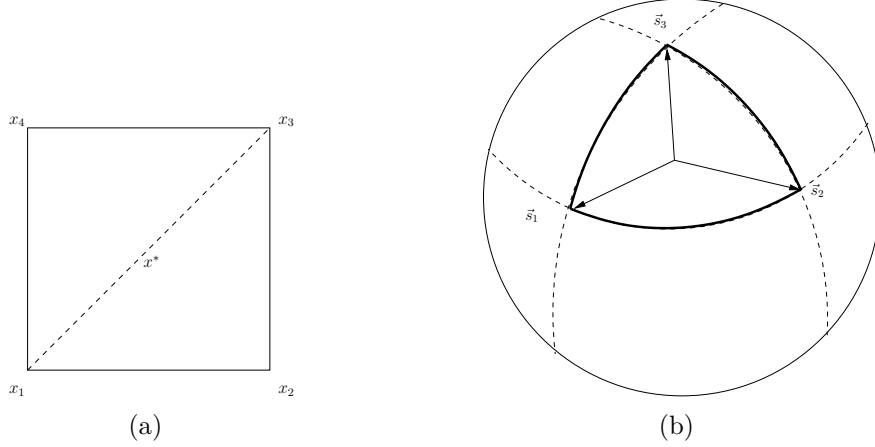


Figure 2: (a) A unit square of the direct lattice, i.e., a site of the dual lattice. (b) Spherical triangle corresponding to the spins  $\vec{s}_1$ ,  $\vec{s}_2$  and  $\vec{s}_3$ .

## 4 Numerical simulations on the lattice

In this Section we describe the setup of our numerical simulations on the lattice, and we discuss our results on the critical behaviour of the two-dimensional  $O(3)_\theta \text{NL}\sigma\text{M}$  at  $\theta = \pi$  at finite lattice spacing.

### 4.1 The $O(3)_\theta \text{NL}\sigma\text{M}$ on the lattice

In order to compute numerically the functional integrals Eq. (8), one replaces the continuum by a square lattice  $\Lambda$  of finite size  $V$ , properly discretising the action. The simplest choice for  $S$  is

$$S[\vec{s}] \rightarrow \frac{1}{g^2} \sum_{x \in \Lambda} \sum_{\mu=1}^2 [1 - \vec{s}(x) \cdot \vec{s}(x + \hat{\mu})] = 2\beta V + \beta S_{\text{latt}}[\vec{s}], \quad \beta = 1/g^2. \quad (30)$$

Here  $\hat{\mu}$  is a unit lattice vector in direction  $\mu$ . The lattice action  $S_{\text{latt}}[\vec{s}]$  is identical to the energy of the Heisenberg statistical model, so that the resulting expression for  $Z(\theta = 0)$  gives (up to an irrelevant constant) the partition function of this model at temperature  $1/\beta$  (in units of the Boltzmann constant). As regards the topological charge, we have used the geometrical definition of Ref. [26],

$$Q_{\text{geom}}[\vec{s}] = \sum_{x^* \in \Lambda^*} q(x^*), \quad q(x^*) = \frac{1}{4\pi} [(\sigma A)(\vec{s}_1, \vec{s}_2, \vec{s}_3) + (\sigma A)(\vec{s}_1, \vec{s}_3, \vec{s}_4)] , \quad (31)$$

where  $x^*$  are sites of the dual lattice  $\Lambda^*$  (i.e., squares of the direct lattice  $\Lambda$ ), and  $\vec{s}_i = \vec{s}(x_i)$  are the spin variables living on the corners  $x_i$  of the squares (ordered

---

<sup>4</sup>This result holds with a milder assumption on the relation between  $\tilde{g}$  and  $\pi - \theta$ , namely that  $\tilde{g} \propto \pi - \theta + \dots$  with subleading terms suppressed with respect to  $\frac{\log \log \frac{1}{\pi - \theta}}{\log \frac{1}{\pi - \theta}}$ .

$\beta$	$V$	statistics
0.9	$100^2$	$2 \cdot 10^6$
1.2	$100^2$	$2 \cdot 10^6$
1.5	$100^2$	$2 \cdot 10^6$
1.6	$200^2$	$4 \cdot 10^6$
1.7	$350^2$	$2 \cdot 10^6$

Table 1: Details of the simulations.

counterclockwise starting from the bottom left corner, see Fig. 2 (a)). Here we have denoted by  $(\sigma A)(\vec{s}_1, \vec{s}_2, \vec{s}_3)$  the signed area of the spherical triangle having as vertices  $\vec{s}_1$ ,  $\vec{s}_2$ , and  $\vec{s}_3$  (see Fig. 2 (b)): the absolute value of the area  $A$  and its sign  $\sigma$ , i.e., the orientation of the spherical triangle, are given respectively by

$$A = \alpha_1 + \alpha_2 + \alpha_3 - \pi, \quad \sigma = \text{sign} [\vec{s}_1 \cdot (\vec{s}_2 \wedge \vec{s}_3)] , \quad (32)$$

with  $\alpha_i$  the angles at the corners of the spherical triangle; the two terms  $q(x^*) = q_1(x^*) + q_2(x^*)$  in Eq. (31) correspond to the two triangles in which each square on the lattice is divided. In terms of the spin variables one has

$$\begin{aligned} \exp \left\{ \frac{i}{2}(\sigma A) \right\} &= \rho^{-1} [1 + \vec{s}_1 \cdot \vec{s}_2 + \vec{s}_2 \cdot \vec{s}_3 + \vec{s}_3 \cdot \vec{s}_1 + i\vec{s}_1 \cdot (\vec{s}_2 \wedge \vec{s}_3)] , \\ \rho^2 &= 2(1 + \vec{s}_1 \cdot \vec{s}_2)(1 + \vec{s}_2 \cdot \vec{s}_3)(1 + \vec{s}_3 \cdot \vec{s}_1) . \end{aligned} \quad (33)$$

Except for the exceptional configurations

$$\vec{s}_1 \cdot (\vec{s}_2 \wedge \vec{s}_3) = 0, \quad 1 + \vec{s}_1 \cdot \vec{s}_2 + \vec{s}_2 \cdot \vec{s}_3 + \vec{s}_3 \cdot \vec{s}_1 \leq 0, \quad (34)$$

for which the topological charge is not defined, one has  $\sigma = \pm 1$  and  $A < 2\pi$ . One verifies directly that  $Q_{\text{geom}}$  has the correct continuum limit; moreover, imposing periodic boundary condition, it necessarily takes only integer values.<sup>5</sup>

Regarding the numerical simulation of the system, the non-linear dependence of  $Q_{\text{geom}}$  on the spins makes it hard to envisage fast algorithms; we have therefore used a simple Metropolis algorithm, supplemented by a “partial overrelaxation” algorithm to accelerate the decorrelation between configuration. This “partial overrelaxation” algorithm simply consists in proposing the usual overrelaxation step used when simulating the model at  $\theta = 0$  to the Metropolis accept/reject step. This algorithm turns out to be rather efficient, especially when  $\beta$  is large and the topological content of configurations changes rarely; notwithstanding its simplicity, it turns out also to be very effective in decorrelating configurations.

---

<sup>5</sup>It is worth mentioning that the Mermin-Wagner-Hohenberg theorem [27, 28, 29], that forbids the possibility of spontaneous magnetisation in the model at  $\theta = 0$ , can be easily extended to  $\theta \neq 0$  if the geometric definition  $Q_{\text{geom}}$  of the charge is used.

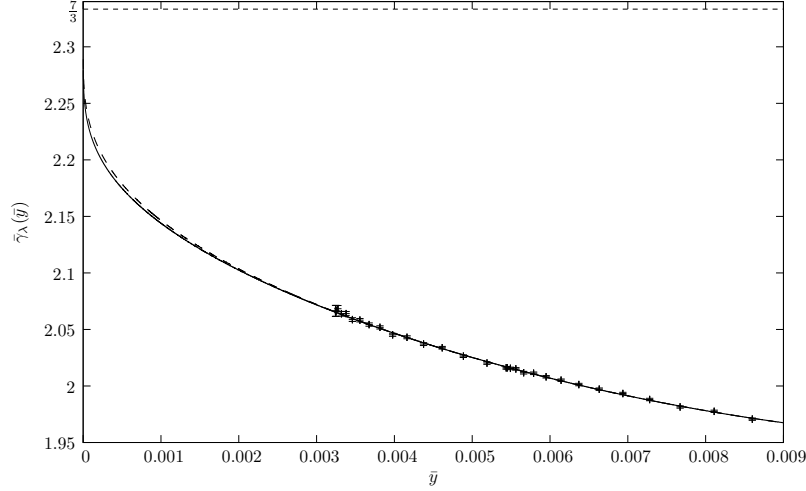


Figure 3: Plot of the effective exponent  $\bar{\gamma}_\lambda(\bar{y})$  for  $\beta = 1.5$ , together with the result of a Bayesian fit at fixed  $\bar{\gamma} = \bar{\gamma}_\lambda(0)$  (solid line, Tab. 2 (left)) and with free  $\bar{\gamma}$  (long-dashed line, Tab. 2 (right)).

## 4.2 Numerical analysis

We have performed numerical simulations of the  $O(3)_\theta \text{NL}\sigma\text{M}$  at various values of the coupling. For each value of  $\beta$  we have chosen 45 values of  $h$ , in such a way that the topological charge was measured for both  $z = \cosh \frac{h}{2}$  and  $z_\lambda = e^{\frac{\lambda}{2}} z \equiv \cosh \frac{h_\lambda}{2}$ ; we used  $\lambda = 0.5$ . The (real) values of  $h = i\theta$  that we used lie below the line of (possible) phase transitions determined in Ref. [30], so that the region where our simulations were performed and the real- $\theta$  axis belong to the same analyticity domain in the complex- $\theta$  plane. The statistical error on the topological charge has been determined through binning. The lattice size was chosen in order for the finite size effects to be negligible (see Tab. 1).

We have then analysed the results for the effective exponent  $\bar{\gamma}_\lambda$  by means of Bayesian fits [31], based on the theoretical prediction described in Section 3.2. In a nutshell, a Bayesian fit takes into account our knowledge (the so-called *priors*) about the parameters that we are fitting. A detailed account of the analysis can be found in Appendix A: here we will mainly discuss the results.

The fits were based on the following general form of  $\bar{\gamma}_\lambda$ ,

$$\bar{\gamma}_\lambda(\bar{y}) = \bar{\gamma} + F \left( \log \frac{\bar{y}_0}{\bar{y}}, \{a_j^{(k)}\} \right), \quad (35)$$

with  $F(x) \rightarrow 0$  as  $x \rightarrow \infty$ , that can be derived from the expected critical behaviour at  $\theta = \pi$  (neglecting terms that vanish as power laws). The values of the parameters  $\bar{y}_0$  and  $a_j^{(k)}$  are not determined by the theoretical analysis, and have been fitted to the lattice data.

A first analysis has been carried out by fixing  $\bar{\gamma}$  to the theoretical value,  $\bar{\gamma} = \frac{7}{3}$ , and fitting the other parameters, starting with  $\bar{y}_0$  only and progressively adding

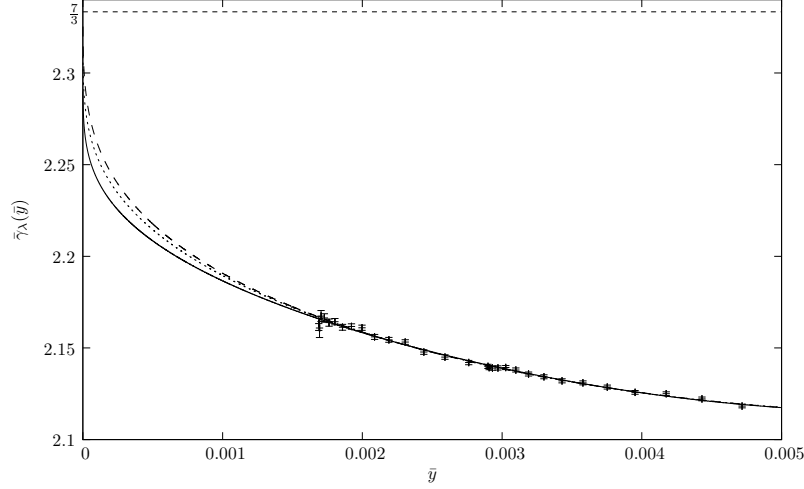


Figure 4: Plot of the effective exponent  $\bar{\gamma}_\lambda(\bar{y})$  for  $\beta = 1.6$ , together with the result of a Bayesian fit at fixed  $\bar{\gamma} = \bar{\gamma}_\lambda(0)$  (solid line, Tab. 3 (left)) and with free  $\bar{\gamma}$  (long-dashed line, Tab. 3 (right), and short-dashed line, Tab. 4).

terms, in order of relevance. We have then used the information obtained on  $\bar{y}_0$  to tune the priors for a second fit, letting all the parameters free to vary. The results are reported in Tabs. 2, 3 and 5, for  $\beta = 1.5$ ,  $\beta = 1.6$  and  $\beta = 1.7$ , respectively. Finally, at  $\beta = 1.6$  we have also tried a fit using information on  $a_0^{(1)}$ , obtained from the fit at fixed  $\bar{\gamma}$ , in order to set the corresponding priors: the results are reported in Tab. 4. The results of the fit with the largest number of parameters are shown in Figs. 3, 4 and 5, for  $\beta = 1.5$ ,  $\beta = 1.6$  and  $\beta = 1.7$ , respectively.

From the results of the analysis described above, we conclude that the lattice data are compatible, within the errors, with the critical behaviour predicted from the WZNW model, at  $\beta = 1.5$ ,  $\beta = 1.6$  and  $\beta = 1.7$ . On the other hand, data at  $\beta = 0.9$  and  $\beta = 1.2$  led to bad-quality fits when fixing  $\bar{\gamma}$  to the theoretical value, and to a value of  $\bar{\gamma}$  considerably smaller than the theoretical prediction when allowed to float ( $\sim 1.9$  for  $\beta = 0.9$ ,  $\sim 2$  for  $\beta = 1.2$ ). This shows that the WZNW-like critical behaviour does not hold at small  $\beta$ , breaking down at some critical value yet to be determined, but does not allow us to draw any conclusion on the details of what happens as one lowers  $\beta$ . The problem is that our analysis *assumes* a given logarithmic factor in the critical behaviour of the topological charge at  $\theta = \pi$ , rather than obtaining it from the numerical data. A few attempts have shown that if we vary the exponent of the logarithmic factor in  $\bar{y}$ , as described in footnote 3, we still obtain a good fit but the value for the critical exponent  $\bar{\gamma}$  resulting from the fit changes, too. For this reason, we have not attempted a more quantitative analysis at  $\beta = 0.9$  and  $\beta = 1.2$ .

Summarising, our results are compatible with one of the two following scenarios.

1. There is a critical value  $\beta = \beta_c$ , above which the critical behaviour of the  $O(3)_\theta \text{NL}\sigma\text{M}$  at  $\theta = \pi$  is exactly the one predicted by the WZNW model at

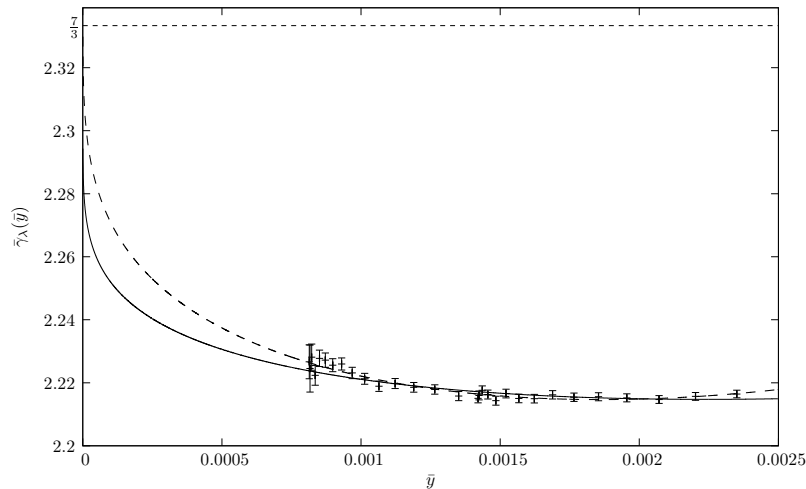


Figure 5: Plot of the effective exponent  $\bar{\gamma}_\lambda(\bar{y})$  for  $\beta = 1.7$ , together with the result of a Bayesian fit at fixed  $\bar{\gamma} = \bar{\gamma}_\lambda(0)$  (solid line, Tab. 5 (left)) and with free  $\bar{\gamma}$  (long-dashed line, Tab. 5 (right)).

topological coupling  $k = 1$ .

2. The critical behaviour becomes exactly the one predicted by the WZNW model only at infinite  $\beta$ , but for  $\beta$  large enough,  $\beta \gtrsim \tilde{\beta}_c$ , the difference is not appreciable numerically.

As for what happens at small  $\beta$ , there are various possibilities. As one expects the system to undergo a first-order phase transition at  $\theta = \pi$  at strong coupling, in the case of the first scenario above there may be a sharp change in the nature of the transition from first order to WZNW-like second order, with the order parameter vanishing at  $\theta = \pi$  as  $\mathbf{O} \propto (\pi - \theta)^\epsilon$  with  $\epsilon = \frac{1}{3}$ . It is however also possible that the nature of the transition changes continuously, i.e., the critical exponent  $\epsilon$  varies from 0 to  $\frac{1}{3}$  as  $\beta$  increases, either reaching  $\frac{1}{3}$  at some finite value of  $\beta = \beta_c$ , or only asymptotically, as in the second scenario above.

## 5 Conclusions

In this paper we have studied the critical behaviour of the two-dimensional  $O(3)$  nonlinear sigma model with  $\theta$ -term ( $O(3)_\theta \text{NL}\sigma\text{M}$ ) at  $\theta = \pi$ , by means of numerical simulations at imaginary  $\theta$ . Using the method of Refs. [20, 21, 22, 23], it is possible in principle to reconstruct the behaviour of the topological charge density for real  $\theta$ , and so investigate the issue of parity symmetry breaking at  $\theta = \pi$ . The theoretical expectation is that parity symmetry is recovered at  $\theta = \pi$  through a second-order phase transition, the behaviour at the critical point being determined by the  $SU(2)$  Wess-Zumino-Novikov-Witten (WZNW) model [13, 14, 15] at topological coupling  $k = 1$ .

Assuming that this is the case, one can show that the method of Refs. [20, 21, 22, 23] is unlikely to yield the correct critical exponent, as the large logarithmic violations to scaling at the critical point make it difficult to reconstruct the critical behaviour from the numerical data. Assuming that the logarithmic violations are known, it is however easy to modify the method in order to overcome this problem. We have then been able to show that our numerical results for sufficiently large  $\beta$ , i.e., for sufficiently weak coupling, are compatible with the expected WZNW-like behaviour at  $\theta = \pi$ , in agreement with previous numerical investigations [2, 16].

Several issues remain open. Although the modified method allows to take care of logarithmic violations, it is necessary to know them in advance in order for it to work properly. Infact, an incorrect assumption on these logarithmic violations could not be detected from the numerical analysis, and so would lead to an incorrect evaluation of the critical exponent. The bottom line is that our modified method can be used to *test* a theoretical expectation on the critical behaviour of a model with results from numerical investigation, but would not lead to conclusive results if one rather tried to *determine* the critical behaviour from the numerical data.

For this reason, we have not been able to determine the critical behaviour of the  $O(3)_\theta \text{NL}\sigma\text{M}$  at smaller values of  $\beta$ , although we have been able to exclude that it is the same as in the WZNW model. Also, due to the numerical errors, we are not able to tell if the critical behaviour is *exactly* WZNW-like, starting from some critical value of  $\beta$ , or if it becomes WZNW-like only *asymptotically*. Further investigations are therefore required, in order to unveil completely the phase diagram of the  $O(3)_\theta \text{NL}\sigma\text{M}$ .

Being in agreement with Refs. [2, 16], the results of this paper are obviously in disagreement with those obtained in Ref. [22] for the  $CP^1$  model. There are basically two possibilities: either the  $O(3)$  and  $CP^1$  model are not equivalent, contrary to the standard wisdom; or they are equivalent, and the results obtained in Ref. [22] are affected by the numerical problems related to the logarithmic violations, discussed in Section 3.2. In order to settle this issue, a new analysis of the numerical data of Ref. [22] is required, along the lines developed in this paper, which will be discussed in a forthcoming publication.

## Acknowledgments

This work was funded by an INFN-MICINN collaboration (under grant AIC-D-2011-0663), MICINN (under grant FPA2009-09638 and FPA2008-10732), DGIID-DGA (grant 2007-E24/2), and by the EU under ITN-STRONGnet (PITN-GA-2009-238353). EF is supported by the MICINN Ramon y Cajal program. MG is supported by MICINN under the CPAN project CSD2007-00042 from the Consolider-Ingenio2010 program.



## A Bayesian analysis

The basic idea behind constrained fits, also called Bayesian fits, is to use the available information on a given physical problem in order to improve the fits to the numerical data. We will not go into the details, that can be found in Ref. [31] and references therein: in this Appendix we will briefly describe the method in order to define the relevant notation and terminology. Then, after slightly extending the theoretical analysis of Section 3.2, we describe its application to the problem at hand.

### A.1 Constrained fits

Constrained fits are performed in practice by minimising a modified chi-squared, the augmented chi-squared  $\chi_{\text{aug}}^2$ , defined as  $\chi_{\text{aug}}^2 = \chi^2 + \chi_{\text{prior}}^2$ , where  $\chi^2$  is the usual chi-squared, and where  $\chi_{\text{prior}}^2$  contains extra information that is used to constrain the fit. If, thanks to prior theoretical knowledge, one expects the parameters to be fitted, call them  $a_1, a_2, \dots, a_n$ , to be close to the values  $\tilde{a}_1, \tilde{a}_2, \dots, \tilde{a}_n$  within the ranges  $\tilde{\sigma}_1, \tilde{\sigma}_2, \dots, \tilde{\sigma}_n$ , then one sets

$$\chi_{\text{prior}}^2 = \sum_{i=1}^n \frac{(a_i - \tilde{a}_i)^2}{\tilde{\sigma}_i^2}. \quad (36)$$

This approach allows to add as many terms to the fitting function as desired, contrary to what happens with standard fits. The goodness of the procedure is judged by the convergence of the errors on the various parameters as the number of terms is increased, and by the value of  $\frac{\chi_{\text{aug}}^2}{n^{\circ} \text{data}}$ , which should be of the order of or smaller than 1. If this is the case, the resulting error at the end of the procedure is expected to give a reasonable estimate of both the statistical and the systematic errors on the parameters of the fit.

### A.2 Subleading terms in the effective exponent

In order to perform a Bayesian analysis of our numerical data, we need to go a few steps further in the derivation of the theoretical prediction for the relevant quantities. Ignoring corrections that contain powers of  $z$ , one can show that the effective exponent  $\bar{\gamma}_\lambda(\bar{y})$  is of the following form,

$$\bar{\gamma}_\lambda(\bar{y}) = \frac{7}{3} \left\{ 1 + \frac{1}{\log \frac{\bar{y}_0}{\bar{y}}} \sum_{k=1}^{\infty} \sum_{j=0}^k Y_j^{(k)}(\lambda) \frac{\left( \log \log \frac{\bar{y}_0}{\bar{y}} \right)^j}{\left( \log \frac{\bar{y}_0}{\bar{y}} \right)^k} \right\}. \quad (37)$$

In order to determine all the coefficients  $Y_j^{(k)}(\lambda)$ , one should know the subleading terms in the relation between the mass gap and the coupling  $\tilde{g}$ , and moreover all the proportionality constants relating  $\tilde{g}$  with  $\pi - \theta$ , the free energy with the squared

mass gap, and so on. However, the coefficients  $Y_k^{(k)}(\lambda)$  are under control, as they are not affected by the subleading terms and by the unknown constants (assuming of course that  $\tilde{g}$  has power, or power/log corrections only, beside the term linear in  $\pi - \theta$ ). Explicitly,  $Y_k^{(k)}(\lambda) = Y_k^{(k)} = (-7/4)^k$ . One can therefore resum the corresponding terms in Eq. (37), obtaining

$$\bar{\gamma}_\lambda(\bar{y}) = \frac{7}{3} \left\{ 1 - \frac{7}{4} \frac{\log \log \frac{\bar{y}_0}{\bar{y}}}{\left(\log \frac{\bar{y}_0}{\bar{y}}\right)^2 + \frac{7}{4} \log \log \frac{\bar{y}_0}{\bar{y}} \log \frac{\bar{y}_0}{\bar{y}}} + \frac{1}{\log \frac{\bar{y}_0}{\bar{y}}} \sum_{k=1}^{\infty} \sum_{j=0}^{k-1} Y_j^{(k)}(\lambda) \frac{\left(\log \log \frac{\bar{y}_0}{\bar{y}}\right)^j}{\left(\log \frac{\bar{y}_0}{\bar{y}}\right)^k} \right\}. \quad (38)$$

Notice that  $Y_j^{(k)}(\lambda) = \left(\frac{7}{3}\right)^k \tilde{Y}_j^{(k)}(\lambda)$ , with the coefficients  $\tilde{Y}_j^{(k)}(\lambda)$  expected to be of order  $\mathcal{O}(10^{-1})$ , as they contain factors of positive powers of  $\frac{3}{4}$ , and also powers of  $\frac{\lambda}{2}$  (recall that we used  $\lambda = 0.5$  in our analysis).

We have then tried a Bayesian fit retaining the first few terms of Eq. (38), namely using the following function,

$$\bar{\gamma}_\lambda(\bar{y}) = \bar{\gamma} \left\{ 1 - \eta \frac{\log \log \frac{\bar{y}_0}{\bar{y}}}{\left(\log \frac{\bar{y}_0}{\bar{y}}\right)^2 + \eta \log \log \frac{\bar{y}_0}{\bar{y}} \log \frac{\bar{y}_0}{\bar{y}}} + \bar{\gamma} f_1(\bar{y}) + \bar{\gamma}^2 f_2(\bar{y}) + \bar{\gamma}^3 f_3(\bar{y}) + \bar{\gamma}^4 f_4(\bar{y}) \right\}. \quad (39)$$

The powers of  $\gamma$  have been chosen so that the coefficients in the functions  $f_i$ ,

$$\begin{aligned} f_1(\bar{y}) &= \frac{a_0^{(1)}}{\left(\log \frac{\bar{y}_0}{\bar{y}}\right)^2}, & f_2(\bar{y}) &= \frac{a_0^{(2)} + a_1^{(2)} \log \log \frac{\bar{y}_0}{\bar{y}}}{\left(\log \frac{\bar{y}_0}{\bar{y}}\right)^3}, \\ f_3(\bar{y}) &= \frac{a_0^{(3)} + a_1^{(3)} \log \log \frac{\bar{y}_0}{\bar{y}} + a_2^{(3)} \left(\log \log \frac{\bar{y}_0}{\bar{y}}\right)^2}{\left(\log \frac{\bar{y}_0}{\bar{y}}\right)^4}, \\ f_4(\bar{y}) &= \frac{a_0^{(4)} + a_1^{(4)} \log \log \frac{\bar{y}_0}{\bar{y}} + a_2^{(4)} \left(\log \log \frac{\bar{y}_0}{\bar{y}}\right)^2 + a_3^{(4)} \left(\log \log \frac{\bar{y}_0}{\bar{y}}\right)^3}{\left(\log \frac{\bar{y}_0}{\bar{y}}\right)^5}, \end{aligned} \quad (40)$$

are at most of order 1, and actually expected to be of order  $\mathcal{O}(10^{-1})$ , as explained above. Here  $\eta = \bar{\gamma}/(\bar{\gamma} - 1)$ : this relation is easily found by substituting  $\bar{\gamma}$  to the value  $\frac{7}{3}$ , obtained for the WZNW model, in the theoretical analysis.

### A.3 Details of the numerical analysis

As already explained in Section 4.2, a first analysis has been carried out by fixing  $\bar{\gamma}$  to the theoretical value,  $\bar{\gamma} = \frac{7}{3}$ , and fitting the other parameters, starting with  $\bar{y}_0$  only and progressively adding terms, in order of relevance. As regards the priors, we assumed a Gaussian distribution for the coefficients  $a_j^{(k)}$ , with central value 0 and  $\sigma \approx 0.1$ , while for  $\bar{y}_0$  we have chosen central value 0 and  $\sigma \approx 2$ . We report in Tabs. 2 (left), 3 (left) and 5 (left) the results for  $\bar{y}_0$  and for the  $\chi^2_{\text{aug}}/n^\circ$  data, for  $\beta = 1.5$ ,  $\beta = 1.6$  and  $\beta = 1.7$ , respectively.

We have then used the information obtained on  $\bar{y}_0$  to tune the priors for a second fit, letting all the parameters free to vary. The central value for  $\bar{y}_0$  was chosen close to the result obtained with the first fit, with  $\sigma$  equal to the corresponding error. The results for  $\bar{\gamma}$  and  $\bar{y}_0$  are reported in Tabs. 2 (right), 3 (right) and 5 (right), for  $\beta = 1.5$ ,  $\beta = 1.6$  and  $\beta = 1.7$ , respectively. At  $\beta = 1.6$  we have also tried a fit in which we have used information on  $a_0^{(1)}$ , obtained from the fit at fixed  $\bar{\gamma}$ , to similarly set the corresponding priors: the results are reported in Tab. 4.

n° par.	$\log \bar{y}_0$	$\frac{\chi^2_{\text{aug}}}{\text{n° data}}$	n° par.	$\bar{\gamma}$	$\log \bar{y}_0$	$\frac{\chi^2_{\text{aug}}}{\text{n° data}}$
1	-2.3078(22)	12	2	2.3032(18)	-2.051(17)	2.1
2	-2.699(13)	.64	3	2.3360(46)	-2.726(48)	.75
3	-2.685(31)	.63	4	2.3339(87)	-2.69(14)	.75
4	-2.65(20)	.63	5	2.3462(91)	-2.42(15)	.62
5	-2.55(25)	.62	6	2.343(11)	-2.38(16)	.61
6	-2.55(26)	.62	7	2.348(12)	-2.36(18)	.60
7	-2.44(28)	.61	8	2.346(11)	-2.25(18)	.57
8	-2.39(32)	.60	9	2.344(13)	-2.23(20)	.56
9	-2.39(32)	.60	10	2.346(15)	-2.24(21)	.56
10	-2.36(34)	.59	11	2.347(14)	-2.21(20)	.55
11	-2.31(34)	.59	12	2.345(12)	-2.19(21)	.55

Table 2: (Left) Result of a Bayesian fit at  $\beta = 1.5$  with  $\bar{\gamma}$  fixed.  
(Right) Result of a Bayesian fit at  $\beta = 1.5$  with  $\bar{\gamma}$  free.

n° par.	$\log \bar{y}_0$	$\frac{\chi^2_{\text{aug}}}{\text{n° data}}$	n° par.	$\bar{\gamma}$	$\log \bar{y}_0$	$\frac{\chi^2_{\text{aug}}}{\text{n° data}}$
1	-1.3427(47)	2.9	2	2.3222(20)	-1.136(40)	2.6
2	0.08(18)	2.2	3	2.3633(61)	-2.935(87)	.62
3	0.13(32)	2.2	4	2.367(10)	-2.99(14)	.60
4	-2.30(34)	1.2	5	2.3711(86)	-2.77(22)	.55
5	-2.59(26)	1.1	6	2.373(10)	-2.79(18)	.55
6	-2.96(40)	1.1	7	2.375(10)	-2.76(21)	.54
7	-2.83(44)	1.1	8	2.374(14)	-2.71(28)	.53
8	-2.69(37)	.99	9	2.375(14)	-2.72(28)	.53
9	-2.80(37)	.95	10	2.377(15)	-2.73(29)	.53
10	-2.82(41)	.95	11	2.377(15)	-2.72(29)	.53
11	-2.69(36)	.93	12	2.378(17)	-2.73(32)	.53

Table 3: (Left) Result of a Bayesian fit at  $\beta = 1.6$  with  $\bar{\gamma}$  fixed.  
(Right) Result of a Bayesian fit at  $\beta = 1.6$  with  $\bar{\gamma}$  free.

n° par.	$\bar{\gamma}$	$\log \bar{y}_0$	$\frac{\chi^2_{\text{aug}}}{\text{n° data}}$
2	2.3050(15)	-2.230(47)	11
3	2.3627(61)	-2.927(88)	.58
4	2.3597(67)	-2.892(91)	.56
5	2.3601(71)	-2.87(19)	.56
6	2.3581(76)	-2.83(19)	.55
7	2.3586(91)	-2.82(21)	.55
8	2.3580(90)	-2.79(23)	.55
9	2.357(10)	-2.77(25)	.55
10	2.357(12)	-2.78(25)	.55
11	2.357(12)	-2.77(26)	.55
12	2.357(13)	-2.76(28)	.55

Table 4: Result of a Bayesian fit at  $\beta = 1.6$  with  $\bar{\gamma}$  free (2).

n° par.	$\log \bar{y}_0$	$\frac{\chi^2_{\text{aug}}}{\text{n° data}}$	n° par.	$\bar{\gamma}$	$\log \bar{y}_0$	$\frac{\chi^2_{\text{aug}}}{\text{n° data}}$
1	0.200(13)	7.3	2	2.3052(28)	1.10(19)	4.8
2	-2.740(52)	1.3	3	2.3654(98)	-3.35(15)	.87
3	-2.63(10)	1.2	4	2.367(11)	-3.35(16)	.85
4	-2.41(21)	1.2	5	2.373(11)	-3.07(19)	.72
5	-2.39(24)	1.2	6	2.373(11)	-3.08(19)	.72
6	-2.30(29)	1.2	7	2.376(12)	-2.99(20)	.68
7	-2.21(29)	1.2	8	2.375(11)	-2.85(21)	.63
8	-2.23(33)	1.2	9	2.375(12)	-2.86(21)	.63
9	-2.18(36)	1.2	10	2.377(12)	-2.83(22)	.62
10	-2.14(36)	1.2	11	2.377(12)	-2.77(22)	.60
11	-2.12(38)	1.1	12	2.375(12)	-2.71(22)	.58

Table 5: (Left) Result of a Bayesian fit at  $\beta = 1.7$  with  $\bar{\gamma}$  fixed.  
(Right) Result of a Bayesian fit at  $\beta = 1.7$  with  $\bar{\gamma}$  free.

## References

- [1] E. Vicari and H. Panagopoulos, Phys. Rept. **470** (2009) 93 [arXiv:0803.1593 [hep-th]].
- [2] W. Bietenholz, A. Pochinsky and U. J. Wiese, Phys. Rev. Lett. **75** (1995) 4524 [hep-lat/9505019].
- [3] J. Plefka, S. Samuel, Phys. Rev. D **56** (1997) 44.
- [4] M. Imachi, S. Kanou, H. Yoneyama, Prog. Theor. Phys. **102** (1999) 653.
- [5] R. Burkhalter, M. Imachi, Y. Shinno, H. Yoneyama, Prog. Theor. Phys. 106 (2001) 613.
- [6] K. N. Anagnostopoulos, J. Nishimura, Phys. Rev. D **66** (2002) 106008.
- [7] J. Ambjorn, K. N. Anagnostopoulos, J. Nishimura, J. J. M. Verbaarschot, JHEP **0210** (2002) 062.
- [8] V. Azcoiti, G. Di Carlo, A. Galante, V. Laliena, Phys. Rev. Lett. **89** (2002) 141601.
- [9] F. D. M. Haldane, Phys. Lett. A **93** (1983) 464.
- [10] F. D. M. Haldane, Phys. Rev. Lett. **50** (1983) 1153.
- [11] I. Affleck, Phys. Rev. Lett. **66** (1991) 2429.
- [12] I. Affleck and F. D. M. Haldane, Phys. Rev. B **36** (1987) 5291.
- [13] J. Wess and B. Zumino, Phys. Lett. B **37** (1971) 95.
- [14] S. P. Novikov, Sov. Math. Dokl. **24** (1981) 222.
- [15] E. Witten, Commun. Math. Phys. **92** (1984) 455.
- [16] M. Bögli, F. Niedermayer, M. Pepe and U. -J. Wiese, JHEP **1204** (2012) 117 [arXiv:1112.1873 [hep-lat]].
- [17] W. Bietenholz, U. Gerber, M. Pepe and U. -J. Wiese, JHEP **1012** (2010) 020 [arXiv:1009.2146 [hep-lat]].
- [18] U. Wolff, Phys. Rev. Lett. **62** (1989) 361.
- [19] B. Alles and A. Papa, Phys. Rev. D **77** (2008) 056008 [arXiv:0711.1496 [cond-mat.stat-mech]].
- [20] V. Azcoiti, G. Di Carlo, A. Galante and V. Laliena, Phys. Lett. B **563** (2003) 117 [hep-lat/0305005].

- [21] V. Azcoiti, G. Di Carlo, A. Galante and V. Laliena, Phys. Rev. D **69** (2004) 056006 [hep-lat/0305022].
- [22] V. Azcoiti, G. Di Carlo and A. Galante, Phys. Rev. Lett. **98** (2007) 257203 [arXiv:0710.1507 [hep-lat]].
- [23] V. Azcoiti, E. Follana and A. Vaquero, Nucl. Phys. B **851** (2011) 420 [arXiv:1105.1020 [hep-lat]].
- [24] I. Affleck, D. Gepner, H. J. Schulz, and T. Ziman, J. Phys. A: Math. Gen. **22** (1989) 511.
- [25] D. Controzzi and G. Mussardo, Phys. Rev. Lett. **92** (2004) 021601 [hep-th/0307143].
- [26] B. Berg and M. Lüscher, Nucl. Phys. B **190** [FS3] (1981) 412.
- [27] N. D. Mermin and H. Wagner, Phys. Rev. Lett. **17**, (1966) 1133.
- [28] P. C. Hohenberg, Phys. Rev. **158** (1967) 383.
- [29] S. Coleman, Commun. Math. Phys. **31** (1973) 259.
- [30] G. Bhanot and F. David, Nucl. Phys. B **251** [FS13] (1985) 127.
- [31] G. P. Lepage, B. Clark, C. T. H. Davies, K. Hornbostel, P. B. Mackenzie, C. Morningstar and H. Trottier, Nucl. Phys. Proc. Suppl. **106** (2002) 12 [hep-lat/0110175].